J|A|C|S
ARTICLES
Published on Web 10/02/2004

Intermolecular π-to-π Bonding between Stacked Aromatic Dyads. Experimental and Theoretical Binding Energies and Near-IR Optical Transitions for Phenalenyl Radical/Radical versus Radical/Cation Dimerizations

David Small, Vladimir Zaitsev, Yousung Jung, Sergiy V. Rosokha, Martin Head-Gordon,* and Jay K. Kochi*

Contribution from the Department of Chemistry, University of California, and Chemical Sciences Division, Lawrence Berkeley National Laboratory, Berkeley, California 94720, and Department of Chemistry, University of Houston, Houston, Texas 77204

Received June 1, 2004; E-mail: mhg@cchem.berkeley.edu; jkochi@uh.edu

Abstract: The high symmetry and stability of phenalenyl systems, both as the planar π-radical (**P•**) and as the π-cation ($\mathbf{P}^+$), are desirable characteristics of prototypical aromatic donor/acceptor pairs that encourage their use as (binary) models for the study of intermolecular interactions extant in stacked molecular arrays. Thus, quantitative ESR spectroscopy of the paramagnetic **P•** identifies its spontaneous self-association to the diamagnetic $\mathbf{P_2}$, previously characterized as the stacked π-dimer by X-ray crystallography. Likewise, the rapid cross-association of **P•** with the closed-shell $\mathbf{P}^+$ leads to the stacked π-dimer cation $\mathbf{P_2}^{\bullet+}$ with the "doubled" ESR spectrum diagnostic of complete (odd) electron delocalization. These π-associations are confirmed by UV−vis studies that reveal diagnostic near-IR bands of both $\mathbf{P_2}$ and $\mathbf{P_2}^{\bullet+}$—strongly reminiscent of intermolecular charge-transfer absorptions in related aromatic (donor/acceptor) π-associations. Ab initio molecular-orbital calculations for the π-dimer $\mathbf{P_2}$ predict a binding energy of $\Delta E_D = -11$ kcal mol^{-1}, which is in accord with the experimental enthalpy change of $\Delta H_D = -9.5$ kcal mol^{-1} in dichloromethane solution. Most importantly, the calculations reproduce the intermonomer spacings and reveal the delicate interplay of attractive covalent and dispersion forces, balanced against the repulsions between filled orbitals. For comparison, the binding energy in the structurally related cationic π-pimer $\mathbf{P_2}^{\bullet+}$ is calculated to be significantly larger with $\Delta E_P \approx -20$ kcal mol^{-1} (gas phase), owing to favorable electrostatic interactions not present in the neutral π-dimer (which outweigh the partial loss of covalent interactions). As a result, our theoretical formulation can correctly account for the experimental enthalpy change in solution of $\Delta H_P = -6.5$ kcal mol^{-1} by the inclusion of differential ionic solvation in the formation of the π-pimer.

Introduction

Columnar stackings of planar systems derived from extended aromatic donors constitute important synthetic objectives of organic materials science, especially for new electrical conductors, molecular magnets, etc.[1,2] Effective interdonor (electronic) communications between such neighboring aromatic moieties are critical requirements that are usually achieved by the coupling of molecular units with unpaired spins,[3] i.e., aromatic π-radicals, π-ion radicals, etc. The bulk properties of these solid-state materials have been successfully approached from the theoretical consideration of macroscopic ensembles.[1,4] However, for closest scrutiny at the molecular level, interdonor interactions need to be separately examined as pairwise (ferromagnetic or antiferromagnetic) interactions of paramagnetic (open-shell) units, either with themselves or with diamagnetic (closed-shell) counterparts.

Intermolecular (electron) delocalization between discrete π-systems was first recognized as aromatic cation-radical associates with their parent (neutral) donors by the appearance of new (charge-resonance) absorption bands in the electronic spectra[5,6] and by "doubling" of well-resolved hyperfine splittings in the ESR spectra.[7] Further studies of paramagnetic π-radicals and ion radicals in the solid state and in solution have revealed their tendency to also undergo facile self-association.[8,9] Accordingly, our objective now is to examine quantitatively the reversible energetics and to understand the basis for such intermolecular π-associations. We choose to focus here on the tricyclic (D_{3h}) phenalenyl system for three important reasons:

(1) (a) Farges, J.-P., Ed. *Organic Conductors: Fundamentals and Applications*; Marcel Dekker: New York, 1994. (b) Williams, J. M. *Organic Superconductors (Including Fullerenes): Synthesis, Structure, Properties and Theory*; Prentice Hall: Englewood Cliffs, NJ, 1992. (c) Ferraro, J. R.; Williams, J. M. *Introduction to Synthetic Electrical Conductors*; Academic Press: Orlando, FL, 1987.

(2) Lahti, P. M., Ed. *Magnetic Properties of Organic Materials*; Marcel Dekker: New York, 1999.

(3) (a) Khodorkovsky, V.; Becker, J. Y. *Organic Conductors: Fundamentals and Applications*; Marcel Dekker: New York, 1994; Chapter 3, p 75. (b) Barclay, T. M.; Cordes, A. W.; Haddon, R. C.; Itkis, M. E.; Oakley, R. T.; Reed, R. W.; Zhang, H. *J. Am. Chem. Soc.* **1999**, *121*, 969. (c) Chi, X.; Itkis, M. E.; Reed, R. W.; Oakley, R. T.; Cordes, A. W.; Haddon, R. C. *J. Phys. Chem. B* **2002**, *106*, 8278. (d) Miller, J. S. *Inorg. Chem.* **2000**, *39*, 4392.

(4) Miller, J. S., Drillon, M., Eds. *Magnetism: Molecules to Materials*; Wiley-VCH: Weinheim, Germany, 2001.

10.1021/ja046770i CCC: $27.50

(i) the highly symmetric diamagnetic cation, the paramagnetic radical, and the diamagnetic anion are all planar and persistent/stable species whose spectroscopic properties are well established,[10,11] (ii) the extended aromatic framework is still amenable to rigorous (ab initio) theoretical computations,[12,13]and (iii) the solid-state (bulk) properties of various derivatives are continuing to attract considerable attention.[14,15] Of particular interest is the intermolecular self-association of phenalenyl radical to form the π-dimer and its cross-association with the diamagnetic phenalenyl cation to form the positively charged radical π-dimer

Chart 1

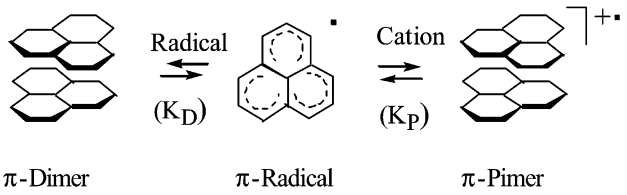

π-Dimer π-Radical π-Pimer

(henceforth referred to as the π-pimer for brevity) in Chart 1. Quantitative evaluation of the energetics of reversible dimerization (K_D) versus pimerization (K_P) in solution is the relevant experimental objective, and the comparative bondings in the two-electron π-dimer versus one-electron π-pimer provide the requisite theoretical underpinnings for an understanding of intermolecular π-associations of open-shell aromatic systems. To facilitate the presentation, the following results are first presented as the experimental measurements and then the theoretical computations of π-dimer/π-pimer bindings.

Experimental Results

The phenalenyl radical for use in this study was quantitatively generated as the 2,5,8-substituted derivative with *tert*-butyl groups to inhibit kinetic lability according to Goto et al.[11,16,17] Indeed, the X-ray crystallographic analysis of this phenalenyl derivative, hereafter designated as **P•**, established the existence of π-dimers in the solid state with interplanar (noncovalent) separations of 3.2−3.3 Å,[11,18] which are too short for a conventional van der Waals complex, but far too long for a conventional chemical bond.

1. Quantitative Evaluations of Phenalenyl π-Dimerization. Two independent spectroscopic methodologies were employed to evaluate quantitatively the reversible dimerization of the phenalenyl radical in dichloromethane solutions according to the temperature-dependent equilibrium

$$\mathbf{P^{\bullet}} + \mathbf{P^{\bullet}} \underset{K_D}{\rightleftharpoons} \pi\text{-}\mathbf{P_2} \qquad (1)$$

A. Temperature Modulation of the ESR Spectrum. The phenalenyl radical (**P•**) in dichloromethane solution exhibits

(5) (a) Lewis, L. C.; Singer, L. S. *Chem. Phys.* **1965**, *43*, 2712. (b) Howarth, O. W.; Fraenkel, G. K. *J. Am. Chem. Soc.* **1966**, *88*, 4514. (c) Howarth, O. W.; Fraenkel, G. K. *J. Chem. Phys.* **1970**, *52*, 6258. (d) Badger, B.; Brocklehurst, B. *Nature* **1968**, *219*, 263. (d) Badger, B.; Brocklehurst, B.; Dudley, R. *Chem. Phys. Lett.* **1967**, *1*, 122. (e) Badger, B.; Brocklehurst, B. *Trans. Faraday Soc.* **1969**, *65*, 2582. (f) Badger, B.; Brocklehurst, B. *Trans. Faraday Soc.* **1969**, *65*, 2588. (g) Badger, B.; Brocklehurst, B. *Trans. Faraday Soc.* **1970**, *66*, 2939. (h) Meot-Ner, M.; Hamlet, P.; Hunter, E. P.; Field, F. H. *J. Am. Chem. Soc.* **1978**, *100*, 5466. (i) Meot-Ner, M. *J. Phys. Chem.* **1980**, *84*, 2724. (j) Meot-Ner, M.; El-Shall, M. S. *J. Am. Chem. Soc.* **1986**, *108*, 4386.

(6) (a) Le Magueres, P.; Lindeman, S.; Kochi, J. K. *J. Chem. Soc., Perkin Trans 2* **2001**, 1180. (b) Kochi, J. K.; Rathore, R, Le Magueres, P. *J. Org. Chem.* **2000**, *65*, 6826. (c) Ganesan, V.; Rosokha, S. V.; Kochi, J. K. *J. Am. Chem. Soc.* **2003**, *125*, 2559.

(7) (a) Gerson, F.; Kaupp, G.; Ohya-Nishiguchi, H. *Angew. Chem., Int. Ed. Engl.* **1977**, *16*, 657. (b) Wartin, A. R.; Valenzuela, J.; Staab, H. A.; Neugebauer, F. A. *Eur. J. Org. Chem.* **1998**, 139. Lau, W.; Kochi, J. K. *J. Org. Chem.* **1986**, *51*, 1801.

(8) (a) Soos, Z. G.; Klein, D. J. In *Molecular Association*; Foster, R., Ed.; Academic: New York, 1975; Vol. 1. (b) Konno, M.; Saito, Y. *Acta Crystallogr.* **1974**, *B30*, 1294. (b) Miller, J. S., Ed. *Extended Linear Chain Compounds*; Plenum Press: New York, 1983; Vols. 2 and 3. (b) Zanotti, G. Del Pra, A.; Bozio, R. *Acta Crystallogr.* **1982**, *B38*, 1225. (c) Vazquez, C.; Calabrese, J. C.; Dixon, D. A.; Miller, J. S. *J. Org. Chem.* **1993**, *58*, 65. (d) Johnson, M. T.; Arif, A. M.; Miller, J. S. *Eur. J. Inorg. Chem.* **2000**, 1781. (e) Novoa, J. J.; Lafuente, P.; Del Seto, R. E.; Miller, J. S. *Angew. Chem., Int. Ed.* **2001**, *40*, 2540. (f) Awere, E. G.; Burford, N.; Haddon, R. C.; Parsons S.; Passmore, J. Waszczak, J. V.; White, P. S. *Inorg. Chem.* **1990**, *29*, 4821.

(9) (a) Hausser, K. H.; Murrell, J. N. *J. Chem. Phys.* **1957**, *27*, 500. (b) Boyd, R. H.; Phillips. *J. Chem. Phys.* **1965**, *43*, 2927. (c) Itoh, M. *Bull. Chem. Soc. Jpn.* **1972**, *45*, 1947. (d) Chang, R. *J. Phys. Chem.* **1970**, *74*, *2029*. (e) Yamagishi, A. *Bull. Chem. Soc. Jpn.* **1975,** *48*, 2440. (f) Bieber, A.; Andre, J. J. *Chem. Phys.* **1975**, *7*, 137. (g) Nakayama S.; Suzuki, K. *Bull. Chem. Soc. Jpn.* **1973**, *46*, 3694. (h) Kimura, M.; Yamada, H,; Tsubomura, H. *J. Chem. Phys.* **1968**, *48*, 440. (i) Itoh, M.; Nagakura, S. *J. Am. Chem. Soc.* **1967**, *89*, 3959. (j) Kosower, E. M.; Cotter, J. L *J. Am. Chem. Soc.* **1964**, *86*, 6, 5524. (k) Sakai, N.; Shirotani, I.; Minomura, S. *Bull. Chem. Soc. Jpn.* **1971**, *44*, 675. (l) Yu, Y.; Gunic, E.; Zinger, B.; Miller, L. L. *J. Am. Chem. Soc.* **1996**, *118*, 1013. (m) Hill, M. G.; Mann, K. R.; Miller, L. L.; Penneau, J.-F. *J. Am. Chem. Soc.* **1992**, *114*, 4, 2728. (n) Hill, M. G.; Penneau, J. F.; Zinger, B.; Mann, K. R.; Miller, L. L. *Chem. Mater.* **1992,** *4*, 1106. (o) Levillain, E.; Ronkali, J. *J. Am. Chem. Soc.* **1999**, *121*, 1, 8760. (p) Lü, J.-M.; Rosokha, S. V.; Kochi, J. K. *J. Am. Chem. Soc.* **2003**, *125*, 12161 (which contains some preliminary results of phenalenyl π-dimerization).

(10) (a) Reid, D. H. *Tetrahedron* **1958**, *3*, 339. (b) Reid, D. H. *Q. Rev.* **1965**, *19*, 274. (c) Reid, D. H. *Chem. Ind.* **1956**, 1504. (d) Gerson, F. *Helv. Chim. Acta* **1966**, *5*, 1463−1467. (e) Sogo, P. B.; Nakazaki, M.; Calvin, M. *J. Chem. Phys.* **1957**, *26*, 1343. (f) Paskovich, D. H.; Reddoch, A. H. *J. Am. Chem. Soc.* **1972**, *94*, 6938. (g) Pogodin, S.; Agranat, I. *J. Am. Chem. Soc.* **2003**, *125*, 12829. (h) Zheng, S.; Lan, J.; Khan, S. I.; Rubin, Y. *J. Am. Chem. Soc.* **2003**, *125*, 5786.

(11) (a) Goto, K.;, Kubo, T.; Yamamoto, K.; Nakasuji, K.; Sato, K.; Shiomi, D.; Takui, T.; Kubota, M.; Kobayashi, T.; Yakusi, K.; Ouyang, J. *J. Am. Chem. Soc.* **1999**, *121*, 1619. (b) Fukui, K.; Sato, K.; Shiomi, D.; Takui, T.; Itoh, K.; Gotoh, K.; Kubo, T.; Yamamoto, K.; Nakasuji, K.; Naito, A. *Synth. Met.* **1999**, *103*, 2257. (c) Morita, Y.; Aoki, T.; Fukui, K.; Nakazawa, S.; Tamaki, K.; Suzuki, S.; Fuyuhiro, A.; Yamamoto, K.; Sato, K.; Shiomi, D.; Naito, A.; Takui, T.; Nakasuji, K. *Angew. Chem., Int. Ed.* **2002**, *41*, 1793. (d) The coordinate system for π-$\mathbf{P_2}$ used in the electronic structure calculations was based on the X-ray structure of the 2,5,8-tri-*tert*-butyl-substituted derivative[11a] in which the two phenalenyl moieties lie parallel to the *x*, *y* plane and are staggered by 60°. (The C_1-to-centroid bond of the lower phenalenyl was arbitrarily placed on the *x*-axis.) (e) The alternative eclipsed conformational isomer of π-$\mathbf{P_2}$ (as in the perchlorinated derivative[14c]) may also be an energy minimum, and we hope to address its electronic structure at a later time.[18c]

(12) (a) Takano, Y.; Taniguchi, T.; Isobe, H.; Kubo, T.; Morita, Y.; Yamamoto, K.; Nakasuji, K.; Takui, T.; Yamaguchi, K. *J. Am. Chem. Soc.* **2002**, *124*, 11122. (b) Takano, Y.; Taniguchi, T.; Isobe, H.; Kubo, T.; Morita, Y.; Yamamoto, K.; Nakasuji, K.; Takui, T.; Yamaguchi, K. *Chem. Phys. Lett.* **2002**, *358*, 17.

(13) Jung, Y.; Head-Gordon, M. *Phys. Chem. Chem. Phys.* **2004**, *6*, 2008−2011.

(14) (a) Chi, X.; Itkis, M. E.; Patrick, B. O.; Barklay, T. M.; Reed, R. W.; Oakley, R. T.; Cordes, A. W.; Haddon, R. C. *J. Am. Chem. Soc.* **1999**, *121*, 10395. (b) Chi, X.; Itkis, M. E.; Kirschbaum, K.; Pinkerton, A. A.; Oakley, R. T.; Cordes, A. W.; Haddon, R. C. *J. Am. Chem. Soc.* **2001**, *123*, 4041. (c) Koutentis, P. A.; Chen, Y.; Cao, Y.; Best, T. P.; Itkis, M. E.; Beer, L.; Oakley, R. T.; Cordes, A. W.; Brock, C. P.; Haddon, R. C. *J. Am. Chem. Soc.* **2001**, *123*, 3864. (d) Pal, S. K.; Itkis, M. E.; Reed, R. W.; Oakley, R. T.; Cordes, A. W.; Tham, F. S.; Siegrist, T.; Haddon, R. C. *J. Am. Chem. Soc.* **2004**, *126*, 1478.

(15) (a) Itkis, M. E.; Chi, X.; Cordes, A. W.; Haddon, R. C. *Science* **2002**, *296*, 1443. (b) Miller, J. S. *Angew. Chem., Int. Ed.* **2003**, *42*, 27. (c) Tomovic, Ž.; Müllen, K. *Angew. Chem., Int. Ed.* **2004**, *43*, 755.

(16) (a) The π-dimers of aromatic radicals and ion radicals are characterized by cofacial sandwich structures (irrespective of overall charge) with interplanar separations of 3−3.6 Å in contrast to σ-dimers in which the two equivalent units are directly connected by a covalent band. (b) Cationic π-pimers[6] are structurally equivalent to the corresponding π-dimer less one electron and akin to the anionic π-pimer[6c] with one additional electron.

(17) (a) Use of bulky *tert*-butyl groups to sterically inhibit σ-dimerization of aromatic radicals was first described by Griller and Ingold: Griller, D.; Ingold, K. U. *Acc. Chem. Res.* **1976**, *9*, 13. (b) It is important to note that the parent phenalenyl radical ($C_{13}H_9$•) cannot be prepared pure owing to the competitive formation of σ-dimers and related (diamagnetic) byproducts.[10]

(18) (a) Such large interannular separations, together with the molecular conformation, suggest that *tert*-butyl groups exert little or no steric effect on the thermodynamics of π-dimerization of **P•** relative to its parent. (b) The cofacial phenalenyl moieties in the π-dimer are staggered (C_6) relative to each other to minimize the steric effects between pairs of interannular *tert*-butyl substituents.[11a] (c) The reversible π-dimerization of phenalenyl radicals relative to their reversible/irreversible σ-dimerization will be reported separately.

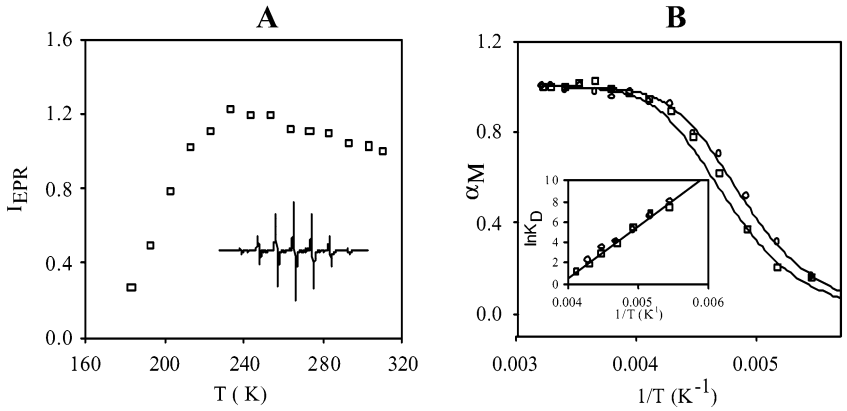

Figure 1. Temperature dependence of (A) the ESR intensity (I_{EPR}) and (B) the monomer fraction (α_M) of the radical **P**• with $c_0 = 2$ mM (○) and 5 mM (□) in CH_2Cl_2. Solid lines: calculated dependencies based on the same concentrations with $\Delta H = -9.5$ kcal/mol and $\Delta S = -36$ eu. Insets: (A) ESR spectrum of **P**•; (B) temperature dependence of the dimerization constant K_D.

well-resolved proton hyperfine splittings in the ESR spectrum initially measured at 23 °C—simply consisting of the binomial septet due to six equivalent aromatic protons with $a_H = 6.2$ G ($g = 2.0028$).[11a] (Both parameters were essentially the same ($a_{6H} = 6.3$ G, $g = 2.0028$) as those of the parent[19] but with additional small quartet splittings of $a_{3H} = 1.8$ G due to the 2-, 5-, and 8-protons.) Upon lowering the temperature, the spectral intensity first increased gradually in the range 310−240 K in accord with the usual Curie−Weiss behavior, and then dropped precipitously as the temperature was further lowered to 180 K (see Figure 1A). Since such temperature-dependent (intensity) changes were quite reversible, and the deviation from Curie−Weiss behavior was more pronounced with increasing initial concentrations of the radical, the major drop in signal intensity was readily assigned to the formation of diamagnetic (ESR-silent) π-dimers according to eq 1. Indeed, the quantitative analysis of the ESR intensity (coupled to appropriate controls) allowed the Curie−Weiss effects to be quantitatively separated from the consequences of changing radical concentrations (see the Experimental Section for details). As a result, the fraction of monomeric radical (α_M) was evaluated directly by double integration of the ESR spectra, and this allowed the dimerization constant $K_D = 0.15 \pm 0.01$ M^{-1} to be calculated at 298 K according to eq 1. The linear dependence of log K_D shown in Figure 1B (inset) afforded the thermodynamic parameters $\Delta H_D = -9.5$ kcal mol^{-1} and $\Delta S_D = -36$ eu at 298 K for the π-dimer.[20]

B. Temperature Modulation of the UV−Vis Spectrum. **P**• in dichloromethane solution appeared pink at room temperature owing to a weak (very broad) absorption band at 595 nm in addition to the principal band at $\lambda_{max} = 540$ nm, $\epsilon_{540} = 103$ mol^{-1} cm^{-1}. Most noteworthy was the dramatic growth of only the 595 nm absorption with decreasing temperature (Figure 2), and its quadratic dependence with changing **P**• concentration at constant temperature was in accord with the dimerization equilibrium in eq 1. Quantitative treatment of the spectral changes (see the Experimental Section) yielded the extinction coefficient of the π-dimer, $\epsilon_D = 2.0 \times 10^4$ mol^{-1} cm^{-1}, and the dimerization constant, $K_D = 0.16 \pm 0.08$ M^{-1}, at 298 K.

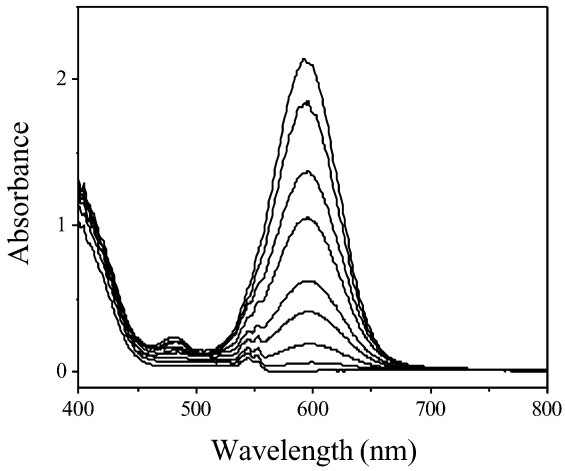

Figure 2. Temperature-modulated spectral changes of the solution of radical **P**• ($c_0 = 5$ mM in CH_2Cl_2). Temperature from bottom to top (°C): 5, −40, −50, −60, −66, −72, −76, −80, −82.

Most importantly, the temperature dependence of the monomer fraction, as determined by such UV−vis spectral measurements, coincided with that derived from the ESR spectral changes at the same concentrations, and the thermodynamic parameters $\Delta H_D = -8.8$ kcal mol^{-1} and $\Delta S_D = -33$ eu were consistent with those evaluated from the ESR data (Figure S1 in the Supporting Information). Thus, independent electronic and ESR spectral methodologies accurately and quantitatively demonstrate (1) the temperature/concentration modulation of the reversible dimerization of **P**• according to eq 1 and (2) the existence of a diamagnetic π-dimer (**P_2**) with the distinctive (strongly allowed) electronic transition at $\lambda_D = 595$ nm ($\epsilon_D = 2.0 \times 10^4$ mol^{-1} cm^{-1}) which is substantially red-shifted relative to that of the parent π-radical monomer with $\lambda_M = 540$ nm ($\epsilon_M = 103$ mol^{-1} cm^{-1}).

2. Quantitative Phenalenyl π-Pimerization with the Diamagnetic Phenalenyl Cation. Intermolecular association of the paramagnetic phenalenyl radical with its closed-shell (cationic) counterpart was quantitatively evaluated as the reversible equilibrium

$$\mathbf{P}^{\bullet} + \mathbf{P}^{+} \underset{K_P}{\rightleftharpoons} \pi\text{-}\mathbf{P}_2^{\bullet+} \qquad (2)$$

by employing the same pair of spectral methodologies in the following way.

(19) The proton hyperfine splittings are $a_{6H} = 6.3$ G and $a_{3H} = 1.8$ G.[10]
(20) For comparison, thermodynamic parameters for σ-dimerization of the parent phenalenyl radical in dichloromethane are $\Delta H_D = -10$ kcal mol^{-1} and $\Delta S_D = -17$ eu.[18c] Close values of these parameters were obtained earlier in toluene ($\Delta H_D = -10$ kcal mol^{-1}, $\Delta S_D = -11$ eu) and in CCl_4 solutions ($\Delta H_D = -11$ kcal mol^{-1}, $\Delta S_D = -15$ eu).[10h]

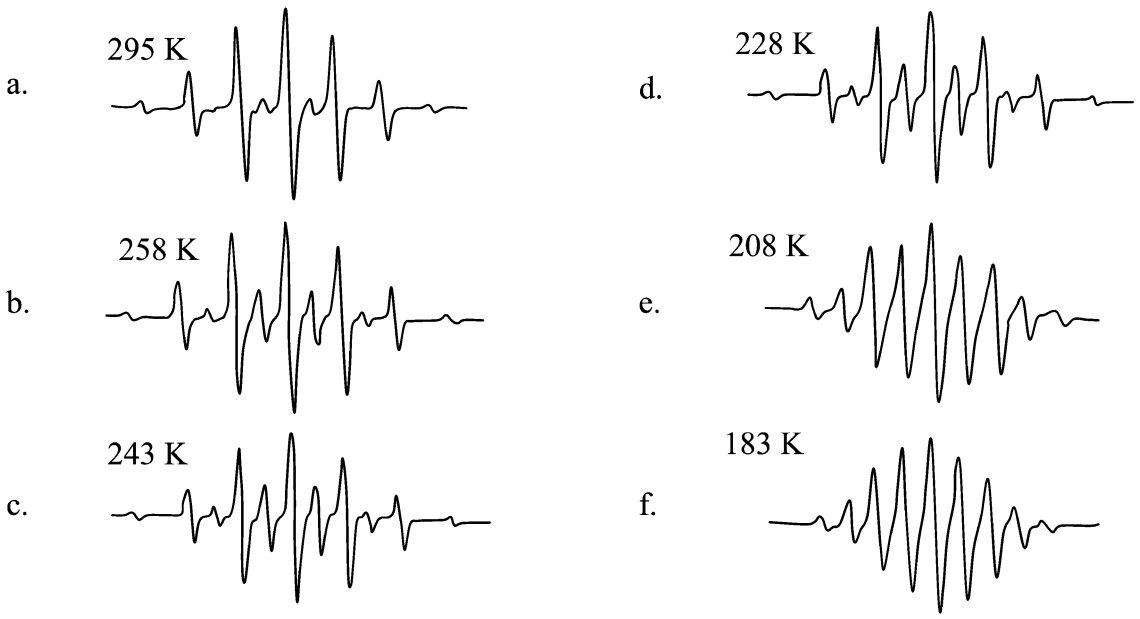

Figure 3. Temperature dependence of the ESR spectrum of an equimolar solution of $\mathbf{P}^{\bullet}$ and $\mathbf{P}^{+}$ in dichloromethane.

A. Doubling of the ESR Spectra in π-Pimerization. The prominent ESR spectrum of a 3 mM solution of $\mathbf{P}^{\bullet}$ in dichloromethane containing an equimolar amount of $\mathbf{P}^{+}$ (as the tetrakis(pentafluorophenyl)borate salt) is shown in Figure 3a as measured at room temperature. However, close scrutiny of Figure 3a revealed the presence of additional lines in the ESR spectrum in addition to the characteristic binomial septet of $\mathbf{P}^{\bullet}$ illustrated in Figure 1A (inset). These new hyperfine lines lay equidistant from the original spectrum of the pure radical, and the line intensities grew dramatically (relative to those of the nearby lines) as the temperature of the solution was progressively lowered as shown in Figure 3b−f. (Essentially the same change in relative line intensities could be reproduced at constant temperature by the incremental addition of $\mathbf{P}^{+}(C_6F_5)_4B^{-}$ to a given concentration of the radical.) Ultimately, all the ESR spectra converged to the final ESR spectrum consisting of the doubling of the number of hyperfine lines with half the hyperfine splittings with the binomial intensity ratio shown in Figure 3f. Such spectral features were readily assigned to the paramagnetic π-dimer cation radical $\mathbf{P_2}^{\bullet+}$, herein to be referred to as the π-pimer. The fraction of the residual $\mathbf{P}^{\bullet}$ radical (α_M), as calculated by double integration of the ESR spectra at various temperatures, is plotted in Figure 4, and it yielded an equilibrium constant of $K_P = 90\ M^{-1}$ for the second-order pimerization in eq 2 at 298 K. The linear dependence of log K_P on (inverse) temperature led to the thermodynamic parameters $\Delta H_P = -6.5$ kcal mol^{-1} and $\Delta S = -13$ eu.

B. Diagnostic Near-IR Bands of Phenalenyl π-Pimers. The addition of the phenalenyl cation, as a $\mathbf{P}^{+}(C_6F_5)_4B^{-}$ salt, to a 3 mM solution of $\mathbf{P}^{\bullet}$ in dichloromethane resulted immediately in the appearance of a new absorption band in the near-IR region with $\lambda_{max} = 1560$ nm (Figure 5), which increased linearly with further incremental additions of salt. Such a near-IR band was diagnostic of the intermolecular π-pimer since neither the phenalenyl radical nor cation alone exhibited any absorption in the low-energy region beyond 1000 nm, even at high concentrations and low temperatures. Furthermore, the progressive lowering of the temperature led to an accompanying absorbance increase similar to that of the 595 nm band of the π-dimer in Figure 2. Indeed, the quantitative analysis of the near-IR spectral changes was successfully carried out (see the Experimental Section for details) for the formation of the paramagnetic phenalenyl π-pimer ($\mathbf{P_2}^{\bullet+}$) with extinction coefficient $\epsilon_P = 9 \times 10^3\ M^{-1}\ cm^{-1}$ and association constant $K_P = 70\ M^{-1}$ at 298 K. The linear dependence of K_D on (inverse) temperature yielded the thermodynamic parameters $\Delta H_P = -5.5$ kcal mol^{-1} and $\Delta S_P = -12$ eu for the π-pimerization according to eq 2. Most importantly, both sets of thermodynamic parameters obtained from the near-IR measurements coincided with those determined from the ESR measurements of the paramagnetic π-pimer, as shown in Figure 4 by the fits of both sets of experimental data to the calculated temperature dependence for the same concentrations based on $\Delta H_P = -6.5$ kcal mol^{-1} and $\Delta S_P = -13$ eu.

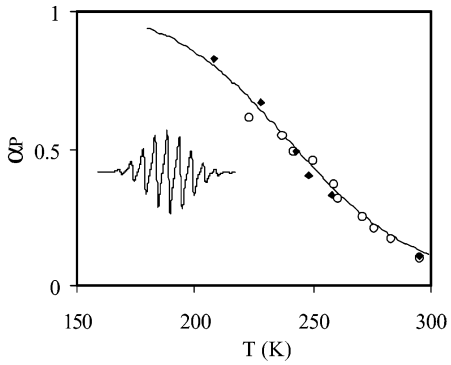

Figure 4. Temperature dependence of the π-pimer $\mathbf{P_2}^{\bullet+}$ fraction (α_P) in solution with an equimolar concentration of radical $\mathbf{P}^{\bullet}$ and cation $\mathbf{P}^{+}$ (3 mM in CH_2Cl_2) as determined from ESR (◆) and electronic (○) spectroscopies. Solid line: calculated dependence based on $\Delta H_P = -6.5$ kcal mol^{-1} and $\Delta S = -13$ eu. Inset: ESR spectrum at 190 K corresponding to the π-pimer $\mathbf{P_2}^{\bullet+}$.

Electronic Structure Calculations

A. General Considerations. In the phenalenyl radical, the singly occupied molecular orbital (SOMO) is composed of six p_z orbitals, with each orbital out of phase with its neighbors as depicted in Chart 2. Owing to the presence of this unpaired

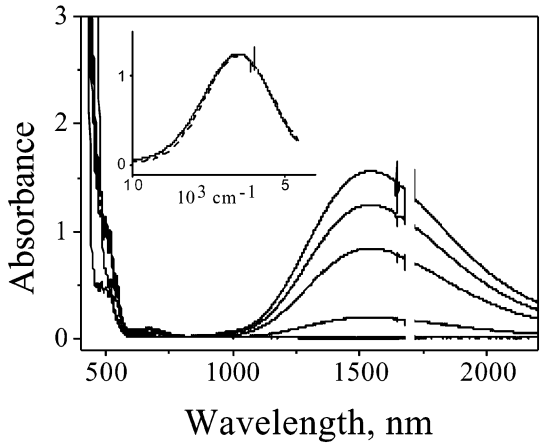

Figure 5. Spectral changes upon incremental addition of cation $\mathbf{P}^+$ to the 1 mM solution of radical $\mathbf{P}^\bullet$ in CH_2Cl_2 at 295 K. Concentration (mM) of $\mathbf{P}^+$ (bottom to top at 1500 nm): 0, 1, 5, 10, 15. Inset: Gaussian deconvolution of the near-IR band.

Chart 2

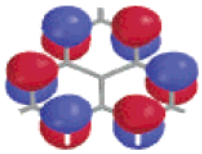

electron, the covalent interactions in the π-dimer $\mathbf{P_2}$[21] resulting from the *intermolecular* π*-dimerization* of phenalenyl radicals derive from the linear combination of the two SOMOs to form π-bonding and π-antibonding orbitals.[11d,22] In addition, such interacting planar organic molecules also inevitably lead to $\pi-\pi$ stacking interactions that largely arise from dynamic electron correlation effects such as dispersion.[12] Although previous theoretical studies[12a,b] have not included dispersion effects (presumably due to computational limitations), we believe that it is the tradeoff between attractive covalent and dispersive interactions and repulsive interactions between the filled levels of each monomer that determines the equilibrium structure. Indeed, the phenalenyl structure is known from solid-state X-ray crystallography[11] to be intermediate between a full π-bond and dissociation, and therefore, the π-dimer is also likely to possess some diradical character,[23,24] which we find interesting to assess quantitatively.

The intermolecular π-pimerization of phenalenyl radical with its diamagnetic cation leads to $\mathbf{P_2}^{\bullet+}$ with a formal bond order of 1/2, and all the interactions described above for the neutral π-dimer will be operative, but the strength of the covalent interactions must necessarily be diminished. However, the π-pimer $\mathbf{P_2}^{\bullet+}$ possesses an additional interaction stemming from its (positive) charge distribution reminiscent of those that are well-known in cation$-\pi$ (benzene) interactions.[25] In such systems, electrostatic interactions between a positive charge and the benzene quadrupole moment are known to be significant. Induction effects are also recognized as very important in cation$-\pi$ interactions.[26] Since phenalenyl radical is more polarizable, and has a higher quadrupole moment than benzene, these electrostatic interactions will surely be operative in $\mathbf{P_2}^{\bullet+}$. It is accordingly very interesting to compare the magnitude and origin of the binding in π-pimer $\mathbf{P_2}^{\bullet+}$ relative to π-dimer $\mathbf{P_2}$. Additionally, the theoretical calculations should account for their distinctly different electronic transitions in the near-IR region (see Figures 2 and 5).

B. Computational Methods. While density functional theory (DFT) calculations[27] are the most common choice for organic molecules, they are not necessarily appropriate for systems such as $\mathbf{P_2}$ and $\mathbf{P_2}^{\bullet+}$ because they do not properly describe dispersion interactions[28] or the separation of charged π-dimers into fragments.[29,30] Caution is also necessary in using wave function methods[31] because of the small HOMO$-$LUMO gap (1.14 eV at the B3LYP/6-31G* level) in $\mathbf{P_2}$. This small gap means that there are important static correlations arising between the HOMO and the LUMO, and the system thus has multireference (or diradicaloid) character. The minimal description of this is a two-configuration self-consistent field wave function, which is equivalent to perfect pairing[32] with one pair, i.e., PP(1). The lowest energy $(N-2)$ electrons are restricted to $(N-2)/2$ spin-paired orbitals, and the remaining two electrons are held in a spin-antisymmetric geminal pair formed from the HOMO and LUMO.

The paramagnetic π-pimer $\mathbf{P_2}^{\bullet+}$ arises from the removal of a single electron from the PP wave function. The resulting $(N-1)$-electron wave function again has $N-2$ electrons in spin-paired orbitals, while the remaining electron is found in a singly occupied (α spin) orbital. This is simply a restricted open-shell Hartree$-$Fock (ROHF) wave function, so this was the starting level of theory chosen for π-pimer $\mathbf{P_2}^{\bullet+}$.

A method for describing the long-range dispersion interactions is also likely to be essential for a system of this type, as shown, for example, in recent studies[13,33] of $K_2(TCNE)_2$, and as is well-known for stacking of closed-shell aromatics such as benzene.[34] Dispersion is largely a result of dynamic electron correlation, and is absent at the PP(1) and ROHF levels of theory. The simplest way in which dispersion can be reincorporated is by performing second-order perturbation theory corrections to PP(1) (as MRMP2[35]) and ROHF (as restricted

(21) For convenience, in the theoretical treatment we employ the same notation (**P**) to denote the parent phenalenyl moiety since its π-bonding behavior is equivalent[18] to that of the *tert*-butyl derivative.
(22) Haddon, R. C. *Aust. J. Chem.* **1975**, *28*, 2343.
(23) (a) Salem, L.; Rowland, C. *Angew. Chem., Int. Ed. Engl.* **1972**, *11*, 92. (b) Dohnert, D.; Koutecky, J. *J. Am. Chem. Soc.* **1980**, *102*, 1789. (c) Borden, W. T.; Iwamura H.; Berson, J. A. *Acc. Chem. Res.* **1994**, *27*, 109.
(24) (a) Jung, Y.; Head-Gordon, M. *ChemPhysChem* **2003**, *4*, 522. (b) Jung, Y.; Head-Gordon, M. *J. Phys. Chem. A* **2003**, *107*, 7475.
(25) (a) Dougherty, D. A. *Science* **1996**, *271*, 163. (b) Ma, J. C.; Dougherty, D. A. *Chem. Rev.* **1997**, *97*, 1303.
(26) Tsuzuki, S.; Yoshida, M.; Uchimaru, T.; Mikami, M. *J. Phys. Chem. A* **2001**, *105*, 769.
(27) Kohn, W.; Becke, A. D.; Parr, R. G. *J. Phys. Chem.* **1996**, *100*, 12974$-$12980.
(28) Kristyan, S.; Pulay, P. *Chem. Phys. Lett.* **1994**, *229*, 175$-$180.
(29) Bally, T.; Sastry, G. N. *J. Phys. Chem. A* **1997**, *101*, 7923$-$7925.
(30) Our first calculations on π-$\mathbf{P_2}$ and π-$\mathbf{P_2}^{\bullet+}$ were based on Kohn$-$Sham DFT using the B3LYP functional, but presumably due to the limitations mentioned above,[28,29] it failed to yield even qualitatively reasonable potential curves, as described in the Supporting Information.
(31) Helgaker, T.; Jorgensen, P.; Olsen, J. *Molecular electronic structure theory*; Wiley: Chichester, U.K., 2000.
(32) (a) Goddard, W. A.; Harding, L. B. *Annu. Rev. Phys. Chem.* **1978**, *29*, 363$-$396. (b) Cullen, J. *Chem. Phys.* **1996**, *202*, 217$-$229. (c) Van Voorhis, T.; Head-Gordon, M. *J. Chem. Phys.* **2002**, *117*, 9190$-$9201.
(33) (a) Jakowski J.; Simons J. *J. Am. Chem. Soc.* **2003**, *125*, 16089. (b) Del Sesto, R. E.; Miller, J. S.; Lafuente, P.; Novoa, J. *Chem.$-$Eur. J.* **2002**, *8*, 4894. (c) Note that, due to the Coulombic repulsion of anion radicals, quantum mechanical calculations lead to net binding within $(TCNE)_2^{2-}$ only in the presence of counterions.[13,33b]
(34) (a) Tsuzuki, S.; Honda, K.; Uchimaru, T.; Mikami, M.; Tanabe, K. *J. Am. Chem. Soc.* **2002**, *124*, 104. (b) Sinnokrot, M. O.; Valeev, E. F.; Sherrill, C. D. *J. Am. Chem. Soc.* **2002**, *124*, 10887. (c) Sinnokrot, M. O.; Sherrill, C. D. *J. Phys. Chem. A* **2003**, *107*, 8377.
(35) Nakano, H. *J. Chem. Phys.* **1993**, *99*, 7983.

MP2[36]). MP2 methods have been shown to be reasonably accurate for calculations of stacking interactions.[34]

Calculations of intermolecular interaction energies are notoriously sensitive to basis set superposition errors (BSSEs). Therefore, we apply a counterpoise correction[37] to the calculations to produce a corrected estimate of the binding energy. Computational limitations restrict the size of the basis set we can apply to 6-31G*, which is considered small for problems of this type, although the extension from 6-31G* to 6-31+G* had little effect in the related $K_2(TCNE)_2$ system.[13]

Electronic excited states were calculated by time-dependent density functional theory (TDDFT), which has been shown to be superior to simple single-excitation CI for most molecular problems.[38] Asymptotic self-interaction problems[39] with TDDFT are avoided by calculating excitation energies only at the equilibrium geometries. Although the lack of dispersion in DFT is an issue for the binding energy, it fortunately does not pose a severe problem for the electronic spectrum calculations.[40]

Binding-energy calculations for the π-pimer $\mathbf{P_2}^{\bullet+}$ and all excited-state calculations were performed using the Q-Chem program,[41] while binding-energy calculations for the π-dimer $\mathbf{P_2}$ were performed using the GAMESS program.[42] Finally, we emphasize that, for computational reasons, all calculations reported here omit the bulky *tert*-butyl groups used in the experimental studies.[18]

C. Binding-energy surfaces were calculated at various **P**-to-**P** separations. At each separation, the geometries were optimized with PP/6-31G* and ROHF/6-31G*, holding the distance between the two central carbons fixed by a Lagrange multiplier constraint.[43] Total energies at each point were calculated with MRMP2 (or MP2) and counterpoise corrected.

1. The Phenalenyl π-dimer surface optimized with PP/6-31G* in Figure 6 shows no minimum, which indicates that covalent interactions alone are insufficient to yield overall binding. By contrast, the highest level of theory, CP-MP2, shows a pronounced minimum in the CP-MP2 surface, which clearly reveals the key role of dispersion in π-dimerization. The calculated binding energy, $\Delta E_D = -11$ kcal mol^{-1}, in the π-dimer is consistent with the experimental value, $\Delta H_D = -9.5$ kcal mol^{-1}. Despite the importance of dispersion in $\mathbf{P_2}$ binding,

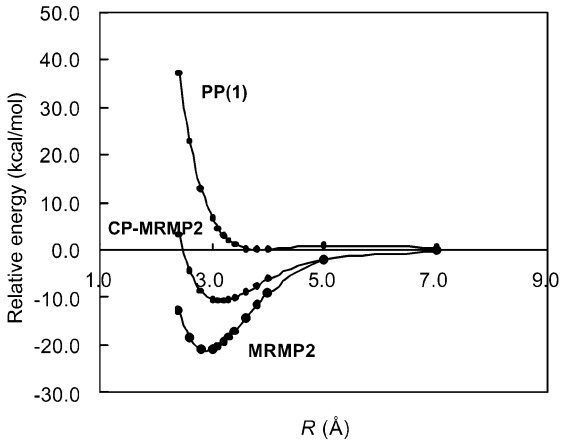

Figure 6. Potential energy surface for the neutral π-dimer as a function of the interplanar separation (*R*). CP-MRMP2 denotes the counterpoise-corrected MRMP2 energies.

Chart 3

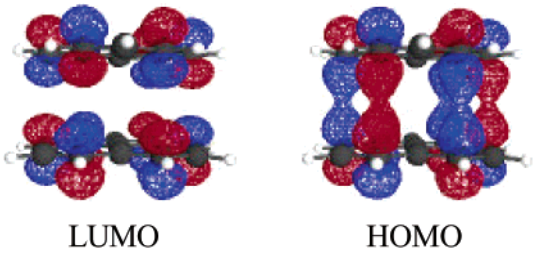

Table 1. LUMO Occupation Numbers of the Neutral π-Dimer $\mathbf{P_2}$ at Different Geometries[11d]

interplanar separation (Å)	occupation number	interplanar separation (Å)	occupation number
2.6	0.15	5	0.95
3.1	0.25	7	1
3.3	0.32		

the interaction is clearly stronger and occurs at significantly shorter distances than conventional π−π stacking of closed-shell aromatic molecules, which are usually separated by van der Waals contact. This difference is attributable to some attractive (SOMO−SOMO) bonding interaction, which is clearly evident, for example, in the correlating HOMO and LUMO for π-$\mathbf{P_2}$ in Chart 3, which shows the monomer SOMOs to be overlapping. Such interactions cannot occur in π−π stacking of closed-shell aromatics. Bonding in the phenalenyl π-dimer can be further understood via the electron occupation number of the PP LUMO (listed in Table 1 for each **P**-to-**P** separation), since it can be used as the criterion for diradical character.[23,24] (For the present purposes, it is sufficient to state that a LUMO occupation number of 1.0 corresponds to a pure diradical, whereas a value of 0.0 indicates a closed-shell species with no diradical character.) As applied to $\mathbf{P_2}$ at the equilibrium point of the CP-MRMP2 curve, the LUMO occupation number according to Table 1 is 0.25, and the π-dimer has 25% diradical character, with 75% bonding character. As such, the nature of the **P**-to-**P** interaction is tantamount to a weak 12-centered covalent bond together with an appreciable (synergistic) dispersion component that stabilizes an otherwise unusually high degree of diradical character. This is quite similar to the $K_2(TCNE)_2$ system that we recently studied.[13]

(36) Knowles, P. J.; Andrews, J. S.; Amos, R. D.; Handy, N. C.; Pople, J. A. *Chem. Phys. Lett.* **1991**, *186*, 130−136.
(37) Boys, S. F.; Bernardi, F. *Mol. Phys.* **1970**, *19*, 553.
(38) (a) Bauernschmitt, R.; Ahlrichs, R. *Chem. Phys. Lett.* **1996**, *256*, 454−464. (b) Hirata, S.; Head-Gordon, M. *Chem. Phys. Lett.* **1999**, *302*, 375−382.
(39) Dreuw, A.; Weisman, J. L.; Head-Gordon, M. *J. Chem. Phys.* **2003**, *119*, 2943−2946.
(40) The impact of dispersion effects is greatly diminished for the following reason. It is typical for the most important excitations to arise from the highest few occupied molecular orbitals and the lowest few virtual orbitals. In contrast, dispersion effects evolve as the cumulative effect of correlations between all the occupied and virtual orbitals. Thus, although the lack of dispersion in DFT is an issue for the binding energy, it does not pose a problem for the spectral calculations.
(41) Kong, J.; White, C. A.; Krylov, A. I.; Sherrill, D.; Adamson, R. D.; Furlani, T. R.; Lee, M. S.; Lee, A. M.; Gwaltney, S. R.; Adams, T. R.; Ochsenfeld, C.; Gilbert, A. T. B.; Kedziora, G. S.; Rassolov, V. A.; Maurice, D. R.; Nair, N.; Shao, Y. H.; Besley, N. A.; Maslen, P. E.; Dombroski, J. P.; Daschel, H.; Zhang, W. M.; Korambath, P. P.; Baker, J.; Byrd, E. F. C.; Van Voorhis, T.; Oumi, M.; Hirata, S.; Hsu, C. P.; Ishikawa, N.; Florian, J.; Warshel, A.; Johnson, B. G.; Gill, P. M. W.; Head-Gordon, M.; Pople, J. A. *J. Comput. Chem.* **2000**, *21*, 1532−1548.
(42) (a) Schmidt, M. W.; Baldridge, K. K.; Boatz, J. A.; Elbert, S. T.; Gordon, M. S.; Jensen, J. J.; Koseki, S.; Matsunaga, N.; Nguyen, K. A.; Su, S.; Windus, T. L.; Dupuis, M.; Montgomery, J. A. *J. Comput. Chem.* **1993**, *14*, 1347−1363. (b) The GAMESS program was used for MRMP2 calculations.
(43) Baker, J. *J. Comput. Chem.* **1997**, *18*, 1079.

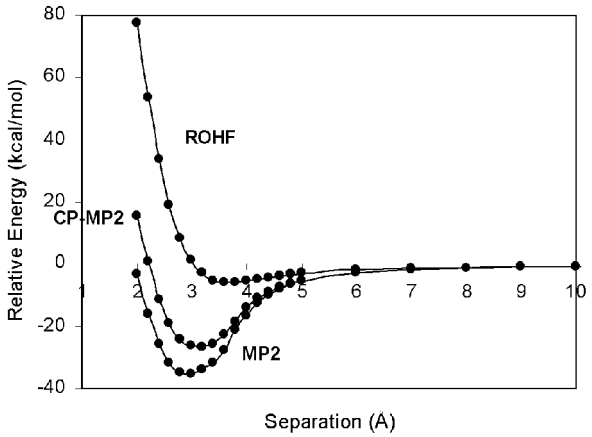

Figure 7. Potential energy surface for the cation π-pimer.

Table 2. TDDFT Results for Low-Lying Electronic Transitions[11d]

	excitation energy (eV)	oscillator strength	transition moment (au)
P_2	2.01	0.2567	0.0002, *X*; −0.0180, *Y*; 2.2845, *Z*
$P_2^{\bullet+}$	1.21	0.1419	0.0001, *X*; 0.0000, *Y*; 2.1862, *Z*
P	2.76	0.0008	−0.0393, *X*; −0.1002, *Y*; 0.0000, *Z*

2. Phenalenyl π-pimer surfaces are bound via both the ROHF and CP-MP2 computations shown in Figure 7. Why is the ROHF curve for $\mathbf{P_2}^{\bullet+}$ bound while the corresponding PP curve for $\mathbf{P_2}$ is not? The answer must be that while covalent effects alone for $\mathbf{P_2}$ are insufficient to yield overall binding (dispersion is required), the *combination* of covalent and electrostatic interactions for $\mathbf{P_2}^{\bullet+}$ is sufficient to yield overall binding. The interaction of permanent and induced moments with positive charge is well-described by Hartree−Fock theory, and comparison of Figures 6 and 7 indicates that these effects are significant. Indeed, cation−π interactions[25] are typically quite strong—with small cations tending to π-bind aromatic donors more tightly than their bulkier counterparts, often with energies that can exceed 10 kcal mol^{-1}. Presumably because of charge delocalization, the calculated binding energy of $\Delta E_P = -6$ kcal mol^{-1} by ROHF/6-31G* is not quite so strong. At the ROHF equilibrium separation of 3.7 Å in the cationic π-pimer, the covalent bonding interaction is weak enough to be considered negligible, and this interaction is largely electrostatic. Dispersion interactions in $\mathbf{P_2}$ and $\mathbf{P_2}^{\bullet+}$ are expected to be roughly comparable,[44] and hence, the monomer fragments are brought closer together in the MP2 calculations, and are more tightly bound, by over 20 kcal mol^{-1}. By contrast with neutral $\mathbf{P_2}$, the dispersion interactions in the cationic $\mathbf{P_2}^{\bullet+}$ are working in concert with two effects: (i) one-electron covalent bonding and (ii) cation−π interaction. The overall result is relatively unusual: the one-electron bond in the cationic π-pimer is *more strongly bound* than the two-electron bond in the neutral π-dimer, because loss of part of the covalent interaction is outweighed by the gain from cation−π interaction.

D. Optical Transition Energies. The results for low-lying electronic transitions obtained at the TDDFT-B3LYP/6-31G* level of theory are summarized in Table 2. In both $\mathbf{P_2}$ and $\mathbf{P_2}^{\bullet+}$, the dominant orbital contribution to the electronic excitation is the HOMO → LUMO transition. This can be seen clearly in an attachment/detachment density analysis.[45] The detachment density is that part of the ground-state density which is promoted and rearranged in the transition, to become the attachment density. Thus, electronic transitions can be visualized as attachment density → detachment density.

Chart 4

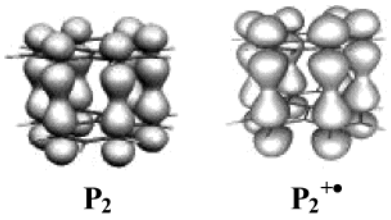

Chart 5

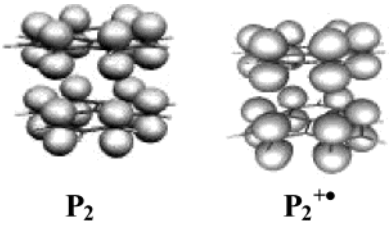

Chart 6

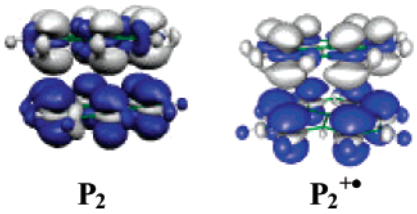

Chart 4 shows that the detachment densities of $\mathbf{P_2}$ and $\mathbf{P_2}^{\bullet+}$ strongly resemble the HOMO of $\mathbf{P_2}$ in Chart 3 (the HOMO for $\mathbf{P_2}^{\bullet+}$ is similar, though not shown). Correspondingly, the attachment densities of $\mathbf{P_2}$ and $\mathbf{P_2}^{\bullet+}$ in Chart 5 are similar to the LUMO also shown in Chart 3.

The experimental red shift in the UV−vis spectra and the stark contrast in absorption intensities between $\mathbf{P_2}$ and $\mathbf{P_2}^{\bullet+}$ are also observed in the TDDFT results. In particular, the excitation energies in Table 2 are in satisfactory agreement with the experimental results shown in Figures 2 and 5 for $\mathbf{P_2}$ and $\mathbf{P_2}^{\bullet+}$, respectively. The transition moments in Table 2 also show that the excitations are markedly dipole-allowed as given by the relative extinction coefficients of $\epsilon_D = 2 \times 10^4$ M^{-1} cm^{-1} and $\epsilon_P = 9 \times 10^3$ M^{-1} cm^{-1}. These experimental results are reinforced in the transition density plots depicted in Chart 6, which show distributions clearly polarized in the direction along the interplanar (**P**-to-**P**) axes.

Discussion

The calculated gas-phase binding energy of −11 kcal mol^{-1} for formation of the π-dimer $\mathbf{P_2}$ is in satisfactory agreement with the experimental value of −9.5 kcal mol^{-1} obtained in dichloromethane solution. On the basis of this agreement, we conclude that the effect of solvation on this π-dimerization is relatively minor. It also supports the view that the bulky *tert*-butyl groups do not significantly impact the energetics of

(44) Dispersion interactions depend primarily on the number of interacting π-electrons, which is 26 and 25 for $\mathbf{P_2}$ and $\mathbf{P_2}^{\bullet+}$, respectively. Thus, their dispersion attractions should be similar.

(45) Head-Gordon, M.; Grana, A. M.; Maurice, D.; White, C. A. *J. Phys. Chem.* **1995**, *99*, 14261−14270.

π-association (apart from the important steric role of inhibiting σ-dimerization).[18,20] From the calculations, the bonding is a weak 12-center covalent interaction (roughly 25% diradicaloid in character), stabilized by dispersion forces, to give an interaction strength 2 or 3 times larger than expected for a van der Waals complex. It is the 75% covalent component that accounts for the preference for antiferromagnetic coupling in the π-dimer seen experimentally.

The enthalpy change for π-dimerization ($\Delta H_D = -9.5$ kcal mol^{-1}) is experimentally found to be significantly larger than the corresponding enthalpy change upon formation of the paramagnetic radical-cation π-dimer $\mathbf{P_2}^{\bullet+}$ ($\Delta H_P = -6.5$ kcal mol^{-1}). On the surface, this difference would appear to reflect the change in π-bonding energies of $\mathbf{P_2}$ versus $\mathbf{P_2}^{\bullet+}$ to parallel the different numbers of frontier electrons involved. Indeed, such a direct conclusion also accords with transition energies ($h\nu_{CT}$) of $\mathbf{P_2}$ (16.5×10^3 cm^{-1}) relative to $\mathbf{P_2}^{\bullet+}$ (6.4×10^3 cm^{-1}) in Figures 2 and 5, respectively.

The theoretical calculations reported above are, however, in qualitative disagreement with this interpretation, because the calculated energy for formation of $\mathbf{P_2}$ (-11 kcal mol^{-1}) is substantially smaller than that of $\mathbf{P_2}^{\bullet+}$ (over -20 kcal mol^{-1}). According to the analysis of the calculations, the stronger binding for $\mathbf{P_2}^{\bullet+}$ versus $\mathbf{P_2}$ is a result of strong stabilizing electrostatic interactions[25] in the radical cation that outweigh the partial loss of covalent interactions. The remaining attractive dispersion interactions are roughly the same[44] for both systems, as are the repulsive Coulomb and exchange interactions between filled orbitals. While the calculations are consistent among themselves, what is the origin of the qualitative discrepancy with experimental observations? The answer, we believe, lies in differential solvation effects on the association energy observed experimentally in dichloromethane solution, but which are omitted from the gas-phase electronic structure calculations. (Separate gas-phase experimental studies of the π-dimers in different charge states would be very desirable to confirm the calculations.)

A rough estimate of the magnitude of differential solvation effects in dichloromethane solvent can be made using the Born model,[46] which accounts for ionic solvation effects to leading order. The Born solvation energy for a unit electronic charge on an ion of radius r in a solvent of dielectric constant ϵ is $\Delta G_S = -(1 - \epsilon^{-1})/2r$. The π-pimer $\mathbf{P_2}^{\bullet+}$ is clearly larger in size and will therefore be more weakly solvated than the combination of separate $\mathbf{P}\bullet$ and $\mathbf{P}^+$. A reasonable estimate of the $\mathbf{P_2}^{\bullet+}$ solute radius is $r \approx 5$ Å. Together with dielectric constant $\epsilon = 9$ for dichloromethane, the solvation energy of $\mathbf{P_2}^{\bullet+}$ will be roughly $\Delta G_S = -30$ kcal mol^{-1}. If the effective radius of $\mathbf{P}^+$ is taken as about two-thirds of that for $\mathbf{P_2}^{\bullet+}$, its solvation energy will then be -44 kcal mol^{-1} to yield an overall solvation-corrected binding energy in qualitative agreement with experiment.

There is also satisfactory agreement between the experimental values of the diagnostic optical transitions in the near-IR region for both $\mathbf{P_2}$ and $\mathbf{P_2}^{\bullet+}$ and the values calculated using TDDFT methods. In this case, solvation corrections for $\mathbf{P_2}^{\bullet+}$ are not expected to be required because they will cancel between the ground and the excited states. Table 3 presents the comparison between the measured and calculated lowest transition energies and relative band intensities. Note the results in Table 3 are arbitrarily normalized to the π-pimer $\mathbf{P_2}^{\bullet+}$, and for the purposes of this study are mainly pertinent to the direct comparison of the properties of $\mathbf{P_2}$ and $\mathbf{P_2}^{\bullet+}$.

Table 3. Near-IR Absorptions for Phenalenyl π-Associations

	energy (eV)		intensity (relative)	
	theor[a]	exptl[b]	theor[c]	exptl[d]
P_2	2.0	2.1	1.9	2.2
$P_2^{\bullet+}$	1.2	0.8	1.0	1.0
P	2.8	2.3	0.006	0.01

[a] HOMO−LUMO excitation energy. [b] Donor/acceptor charge-transfer energy. [c] Oscillator strength. [d] Extinction coefficient.

Summary and Conclusions

Intermolecular π-associations in phenalenyl systems in the form of bimolecular radical/radical and radical/cation interactions lead to the diamagnetic π-dimer $\mathbf{P_2}$ and the cationic (open-shell) π-pimer $\mathbf{P_2}^{\bullet+}$, respectively. Satisfactory agreement is obtained between experimental measurements and theoretical calculations for $\mathbf{P_2}$ only when both covalent and dispersive attractions are included in the latter. The π-binding is thus characterized by a weak, (25%) diradicaloid covalent interaction, stabilized by attractive dispersion interactions, giving an (experimental) enthalpy of formation of $\Delta H_D = -9.5$ kcal mol^{-1}. This interaction is fascinating as it lies between normal van der Waals complexes and normal chemical bonds in strength and properties.

The difference in π-binding (and bonding) between diamagnetic $\mathbf{P_2}$ and paramagnetic $\mathbf{P_2}^{\bullet+}$ emerges as a most intriguing interplay of several factors. According to the gas-phase calculations, loss of covalent character in the π-pimer $\mathbf{P_2}^{\bullet+}$ (a nominal one-electron bond) relative to π-dimer $\mathbf{P_2}$ (a nominal two-electron bond) is outweighed by strong stabilizing electrostatic interactions in the π-pimer that are absent in the neutral π-dimer. Thus, the π-pimer $\mathbf{P_2}^{\bullet+}$ is more strongly bound by theory,[47] but experimentally the opposite is observed in dichloromethane solution. This apparent discrepancy is resolved by considering ionic solvation effects, which more strongly stabilize $\mathbf{P}^+$ relative to $\mathbf{P_2}^{\bullet+}$ owing to its more compact size. As a result, we expect that, in the absence of solvation such as in stacked phenalenyl (solid-state) arrays, the principal electronic communication will occur between neighboring radical/cation centers relative to the competitive annihilation of radical/radical pairs.

It is a challenge for the future, with substantial relevance to the rational design of organic materials with controllable spin couplings, to consider tuning the interactions identified here by altering the size of the stacked aromatic species, as well as the substituents employed at the 2-, 5-, and 8-positions. Larger aromatic donors will lead to stronger π stacking energies, while the strength of covalent interactions can almost certainly be influenced by the choice of substituent, as well as the overall symmetry of the aromatic framework.

Experimental Section

Materials and Synthesis. Chloranil (Aldrich) was purified by repeated recrystallization. 2,5,8-Tri-*tert*-butylphenalene was synthesized

(46) Tomasi, J.; Persico, M. *Chem. Rev.* **1994**, *94*, 2027.

(47) (a) A similar situation exists with the alkali-metal dimers such as Na_2 versus Na_2^+ and K_2 versus K_2^+, and theoretically ascribed to the unfavorable concentration of the valence-electron charge within the ion cores.[47b] (b) Roach, A. C.; Baybutt P. *Chem. Phys. Lett.* **1970**, *7*, 7. (c) Compare also Esterhuysen, C.; Frenking G. *Theor. Chem. Acc.* **2004**, *111*, 381.

according to a literature procedure and identified by its ^{1}H NMR spectrum, GC/MS analysis, and melting point.[10,11] **P**$^\bullet$ was prepared via a modified literature method[11] by reaction of phenalene precursor and chloranil (2:1 molar ratio) in benzene under air-free conditions, followed by extraction of radical **P**$^\bullet$ formed with degassed pentane. Evaporation (in vacuo) of the clear, slightly blue-colored pentane solution afforded radical **P**$^\bullet$ as deep blue needles in 59% yield. Mp: 230 °C dec. UV−vis (hexane): λ_{max} (ϵ) = 545 (100), 392 (330), 374 (4540), 341 (27300), 298 (3130). To synthesize cation **P**$^+$, 300 mg (0.33 mmol) of triphenylcarbenium perfluorotetraphenylborate (from Asahi Glass Co., Ltd.) in 2 mL of CH_2Cl_2 was added under argon to the solution of 2,5,8-tri-*tert*-butylphenalene (140 mg, 0.42 mmol) in 4 mL of CH_2Cl_2. Subsequent addition of 8 mL of hexane to the reaction mixture resulted in precipitation of red crystals, which were separated and recrystallized from ether/hexane (1:2) to afford red needles of **P**$^+$B$(C_6F_5)_4^-$. Yield: 0.20 g (62%). Mp: 264 °C dec. UV−vis (CH_2Cl_2): λ_{max} (ϵ) = 519 (660), 502 (730), 485 (815), 468(800), 423 (4500), 260 (22500). ^{1}H NMR ($CDCl_3$): δ 1.58 (s, 27H, *t*-Bu), 9.15 (s, 6H). X-ray analysis confirmed the structure of **P**$^+$B$(C_6F_5)_4^-$ (Figure S2 in the Supporting Information).

ESR measurements were performed on either a Bruker ESR-300 X-band or a Varian E-line Century 100 ESR spectrometer from +20 to −90 °C in the EPR tube with a Teflon valve under an argon atmosphere. The intensity of the ESR signals, I_{EPR}, was determined by double integration of the averaged spectra after baseline correction. The fraction of monomers, α_M, in the solution of **P**$^\bullet$ was determined from I_{EPR} (normalized as described earlier[9p] to account for the temperature variation related to the Curie law and instrumental factor). The equilibrium constant K_D was calculated as $K_D = (1 - \alpha_M)/2c_R\alpha_M^2$, where c_R is the overall concentration of **P**$^\bullet$ added to solution, and the thermodynamic parameters for dimerization were calculated by the least-squares procedure from the (linear) dependence of ln(K_D) on 1/T. The ESR spectra of the solutions containing both radical **P**$^\bullet$ and cation **P**$^+$ represent superposition of the spectra of monomer **P**$^\bullet$ and π-pimer $\mathbf{P_2}^{\bullet+}$. The fractions of monomer, α_M, in such systems were calculated (i) by computer simulation via the addition of (digitized) spectra of pure monomer and π-pimer and variation of their fractions until the best correspondence with experimental spectra were obtained and (ii) from the ratio of the intensities of the central line in the ESR spectra (which is determined by the sum of the concentrations of monomer and π-pimer) to the intensities of the closest line, which appeared upon addition of cation and is related to the concentration of π-pimer alone (both methods of calculation agreed within 5%). On the basis of α_M, the equilibrium constant of π-pimer formation was calculated as $K_P = (1 - \alpha_M)/[(c_C - \{1 - \alpha_M\}c_R)\alpha_M]$, where c_C and c_R are the overall concentrations of cation and radical added to the solution. The (linear) dependence of ln(K_P) on 1/T afforded thermodynamic parameters ΔH_P and ΔS_P .

Electronic spectroscopy was carried out on an HP 8453 spectrophotometer or a Cary 500 spectrometer using a Dewar equipped with a quartz lens and a cell equipped with a Teflon valve fitted with Viton O-rings as described earlier.[9p] The band at ~595 nm was assigned to π-dimer $\mathbf{P_2}$ on the basis of quantitative treatment of the UV−vis spectral changes (the band intensity was proportional to the square of the radical concentration and increased reversibly with the lowering of the temperature). This assignment was supported by comparison of electronic spectroscopy in solution with the results of the EPR spectral studies, X-ray crystallography, and solid-state electronic spectroscopy. The extinction coefficient (ϵ_D) and thermodynamic parameters (K_D, ΔH_D, ΔS_D) for dimerization were calculated by an approximation method based on the measurement of the intensity of the absorption of the pure π-dimer band with a maximum at 595 nm. The procedure included the variation of the extinction coefficient and the thermodynamic parameters to minimize the difference between the experimental and calculated values of the absorption at λ_L: $\Delta = \Sigma(A^i_{exptl} - A^i_{calcd})^2$. Experimental values of A^i_{exptl} were measured at different temperatures and initial concentrations, and $A^i_{calcd} = e_L l c_D = e_L l[(4K_D c_0 + 1) - (8K_D c_0 + 1)^{0.5}]/8K_D$, with $K_D = \exp[-(\Delta H_D - T\Delta S_D)/RT]$ and l = 0.1 cm. The reliability of the thermodynamic parameters obtained in this way was confirmed by the independent ESR measurements based on the fraction of monomeric radical (vide supra).

Acknowledgment. V.Z., S.V.R., and J.K.K. (Houston) thank the R. A. Welch Foundation and the National Science Foundation for financial support. M.H.-G., D.S., and Y.J. (Berkeley) were supported by the Director, Office of Energy Research, Office of Basic Energy Sciences, Chemical Sciences Division of the U.S. Department of Energy under Contract DE-AC03-76SF00098, supercomputer time from NERSC, and Grant CHE-9981997 from the National Science Foundation.

Supporting Information Available: Temperature dependence of the monomer fraction of radical **P**$^\bullet$ determined by ESR and electronic spectroscopy (Figure S1), X-ray structures of tri-*tert*-butyl-substituted phenalenyl cations (Figure S2), and results of the DFT calculations (B3LYP/6-31G*): potential energy surfaces for the neutral π-dimer $\mathbf{P_2}$ (Figure S3) and for the cationic π-pimer $\mathbf{P_2}^{\bullet+}$ (Figure S4) (PDF).[30] This material is available free of charge via the Internet at http://pubs.acs.org.

JA046770I